PCCP

Photophysical properties of tris(bipyridyl)ruthenium(II) thin films and devices

K. W. Lee,[a] J. D. Slinker,[b] A. A. Gorodetsky,[b] S. Flores-Torres,[a] H. D. Abruña,[a] P. L. Houston[a] and G. G. Malliaras[b]

[a] *Department of Chemistry and Chemical Biology, Cornell University, Ithaca, NY, USA*
[b] *Department of Materials Science and Engineering, Cornell University, Ithaca, NY, USA*

Received 24th February 2003, Accepted 10th April 2003
First published as an Advance Article on the web 8th May 2003

Absorption and luminescence spectra as well as luminescence lifetimes have been measured for $Ru(bpy)_3^{2+}$ in solution and in thin films of varying thicknesses, and these properties have been correlated with the efficiency of organic light emitting devices (OLEDs) made of the films. The lifetimes decrease for films below about 50 nm in thickness but are relatively constant for thicknesses above about 100 nm. This behavior is consistent with a model in which quenching is caused both by intrinsic properties of the molecules and by Förster energy transfer between chromophores that carries the excitation to surface layers, where the excitation is more efficiently quenched. The external quantum efficiency of the OLEDs is also found to increase with thickness, approaching 1% for thicknesses near 200 nm.

1. Introduction

Because they may have economic and fabrication advantages when compared to their inorganic semiconductor counterparts, organic light emitting diodes (OLEDs) have recently received increased attention. Those containing transition metal complexes appear to be particularly promising candidates.[1–4] In particular, tris-chelated 1,2-diimine transition metal ion complexes (especially group VIII: Ru^{2+}, and Os^{2+}) possess attractive advantages over polymers and other small molecules that have been widely used for OLED applications. They have relative ease of synthesis and purification, electronic stability enhanced by the symmetrical t_{2g}^6 configuration, high photoluminescence (PL) quantum yields, moderately long excited state lifetimes, and chemical stability.[5] Among these complexes, $Ru(bpy)_3^{2+}$ (bpy denotes 2,2′-bipyridine) has been studied most extensively. In an acetonitrile solution, a PL quantum yield of *ca*. 6.1% is obtained at room temperature.[5] $Ru(bpy)_3^{2+}$ also shows both metal and ligand based stable and reversible reduction/oxidation behavior and has, therefore, been employed as a material in solution electro-generated chemiluminescence (ECL) cells, where a fairly high quantum efficiency, up to 25%, has been observed.[6] In solution ECL cells containing $Ru(bpy)_3^{2+}$ as well as most other luminescent transition metal complexes, the light emission is phosphorescence from a spin-forbidden (triplet) excited state.[7] Simple spin statistics dictate that the formation of triplet states is three times more efficient than that of singlet states.[8] Moreover, the spin-allowed (singlet) excited states of $^1Ru(bpy)_3^{2+}*$ are rapidly deactivated *via* spin–orbit coupling, leading to the generation of the lowest energy (triplet) excited states.[7] These PL and ECL properties have provided strong motivation for solid-state OLED applications. In addition, when using $Ru(bpy)_3(PF_6)_2$, a single-layer device can be fabricated because $Ru(bpy)_3^{2+}$ can function as both an efficient hole/electron transporter and a light-emitter. The accumulation/depletion of negative counter ions, *e.g.*, PF_6^-, near the anode/cathode facilitates the injection of holes and electrons regardless of the electrode's work function; the contacts are thus ohmic.[4] Rubner *et al.* have realized highly bright and efficient solid-state OLEDs based on $Ru(bpy)_3(PF_6)_2$.[1,2] Their single-layer devices operated at a voltage as low as 2.5 V and showed luminescence levels as high as 1000 cd cm^{-2} at 5 V with an external quantum efficiency on the order of 1%.[1] These researchers also succeeded in lowering the device turn-on time by using different counter ions and thus enhancing ion mobility.[2]

Understanding of the electrochemical processes in ECL cells helps to describe the operational mechanism of solid-state OLEDs based on $Ru(bpy)_3(PF_6)_2$ and other transition metal complexes.[4,8] Once a voltage is applied to the OLED, oxidation of $Ru(bpy)_3^{2+}$ at the anode generates $Ru(bpy)_3^{3+}$, where the additional charge is localized mainly at the metal center. At the cathode, the reduced species, $Ru(bpy)_3^{1+}$, is formed *via* ligand based reduction. Through charge migration and electron transfer, $Ru(bpy)_3^{3+}$ and $Ru(bpy)_3^{1+}$ react by electron transfer recombination to generate the triplet state, $^3Ru(bpy)_3^{2+}*$, which is responsible for the emission observed in conventional ECL cells. The device efficiency is thus related to the PL properties of the Ru complex layer. Recently, Bernhard *et al.* have revealed that the external electroluminescence (EL) efficiency of a device is governed by the PL efficiency of the material.[4] The work described below, which investigates the photophysical properties of $Ru(bpy)_3(PF_6)_2$ thin films on quartz glass plates, reports the fabrication and testing of EL devices with varying thickness. These provide an insight into photophysics in thin films, leading to better strategies for OLED design.

2. Experiment

$Ru(bpy)_3(PF_6)_2$ was prepared in two different ways.[9] First, a mixture of 2,2′-bipyrdine (3.3 mmol) and ruthenium(III) chloride hydrate (0.207 g, 1.0 mmol) in 25 ml of ethylene glycol was refluxed in a microwave oven for 16 min. Water (150 ml) was added to the reaction mixture, and the excess ligand in the orange solution was removed through an extraction with ether (6×50 ml). A water solution of 2.0 g NH_4PF_6 was added,

 DOI: 10.1039/b302119j

which led to the formation of a precipitate. The precipitate was filtered off, rinsed with water, and dried. The complex was purified through vapor diffusion crystallization with acetonitrile/diethyl ether with a yield of *ca.* 80%. In a second procedure, the compound $Ru(bpy)_3Cl_2$ was purchased from Aldrich, and was precipitated with NH_4PF_6. It was then recrystalized and purified following the method described above.

The fabrication of the OLEDs has been described previously.[4] Prior to spin-casting, the quartz plates and pre-patterned indium tin oxide (ITO) substrates were cleaned using deionized water. They were then dried and treated with UV/ozone. An acetonitrile solution of $Ru(bpy)_3(PF_6)_2$ was spin-cast onto the quartz plates and substrates. Afterwards the samples were dried under vacuum. $Ru(bpy)_3(PF_6)_2$ single layers with thicknesses in the range from 15 to 200 nm were prepared by varying the concentration of the solution (16–48 mg mL^{-1}) and spin-speed (1000–5000 rpm). The thicknesses were measured *via* profilometry.

UV-VIS absorption spectra of the thin film samples were obtained using a HP 8453 diode array spectrometer at room temperature. A quartz plate was used as a blank. PL spectra at room temperature were obtained using a SPEX 1681 Minimate-2 spectrofluorimeter with a Spectra Acq CPU controller. Excitation light with a wavelength of 450 nm was incident on the plate at an angle of 45° with respect to the normal axis of a sample plate. PL spectra were collected at normal incidence.

In order to measure lifetimes, an excimer laser (Lambda Physik LPX-205i, 308 nm, 10 Hz) was used to pump a dye laser. The 450-nm output of the dye laser was used to excite the samples. Excitation light was incident on the plate at an angle of 45° with respect to the normal axis of the sample plate. Fluorescence at 610 nm was collected along the normal axis of a sample plate using a 2″ collection lens, a focusing lens, a filter (RG590), and a monochromator equipped with photomultiplier tube (Hamamatsu E990-07). A Lecroy digital oscilloscope was used to collect the data.

3. Results and discussion

A. Photophysics of $Ru(bpy)_3(PF_6)_2$ thin films

Fig. 1 shows the UV-VIS absorption and PL spectra of $Ru(bpy)_3(PF_6)_2$ in an acetonitrile solution and in a 17-nm thin film sample.[10] The similarity of these two spectra indicates that the optical properties of the compound are not changed significantly by the phase of the sample. The peaks in absorption near 290 nm are ascribed to ligand-to-ligand (LL) π–π* transitions, and the second features peaking near 455 nm are assigned as the transition to the singlet metal-to-ligand (d–π*) charge transfer (MLCT) state.[5] The electroluminescence spectrum of the single layer device was found to resemble the PL spectrum of the thin film sample,[4] in agreement with the thesis that phosphorescence from the triplet MLCT state is the source of emission in the OLED device. The absorption peaks are red-shifted in very thin samples. Samples thicker than 120 nm were found to have absorption bands peaking at 292 (π–π* transition) and 453 nm (d–π* transition). On the other hand, the absorption bands of the thinnest sample (d = 17 nm) peaked at 293 and 458 nm. These shifts indicate that thinner samples are affected more by the interactions at interfaces. The PL band, however, was found to remain invariant. The absorptions due to the π–π* transitions and the singlet MLCT transitions were found to be linearly dependent on thickness (Fig. 2), indicating that the samples were made uniformly.

Lifetime profiles are shown in Fig. 3. Each profile was fitted well with two exponential functions with r^2 values in the range of 0.99 through 1.01 while the profile of a solution sample was fitted by a single exponential function. This implies that at least two different decay processes are involved in nonradiative decay. This is not surprising because two quenching processes can be available in this system. According to Haynes *et al.*, the Förster energy transfer (FET) mechanism is mainly responsible for the nonradiative decay process in a thin film environment.[11] Since this type of energy transfer can occur through dipole–dipole interactions between a molecule and the surface, two interfaces of inorganic/glass and inorganic/air should be taken into account.

The lifetime of a medium is expressed as:

$$\frac{1}{\tau_m} = \frac{1}{\tau_r} + k_{nr},$$

where τ_m and τ_r indicate the experimentally measured lifetime in the medium and the lifetime of the emitting molecule in the absence of any nonradiative processes, respectively. k_{nr} is the

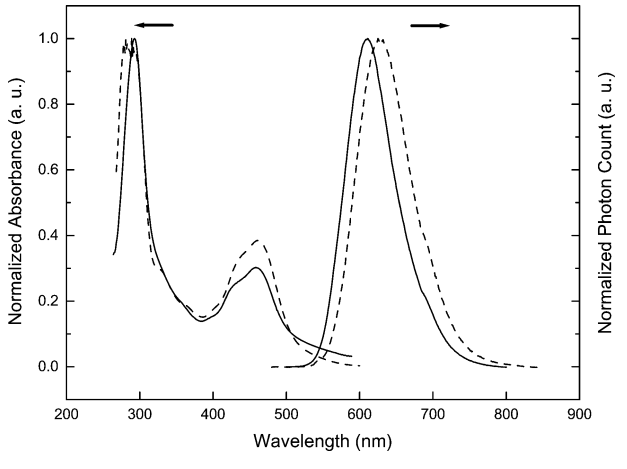

Fig. 1 UV/VIS absorption and PL spectra of $[Ru(bpy)_3](PF_6)_2$ in a 17-nm thin film sample (solid lines) and in an acetonitrile solution (dashed lines).

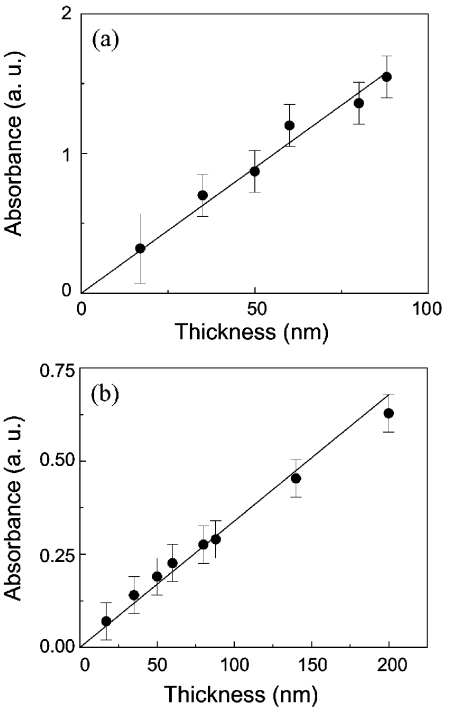

Fig. 2 Peak absorbance of the (a) LL (π–π*) and (b) MLCT (d–π*) transitions as a function of film thickness. The solid lines represent linear fits to the data points.

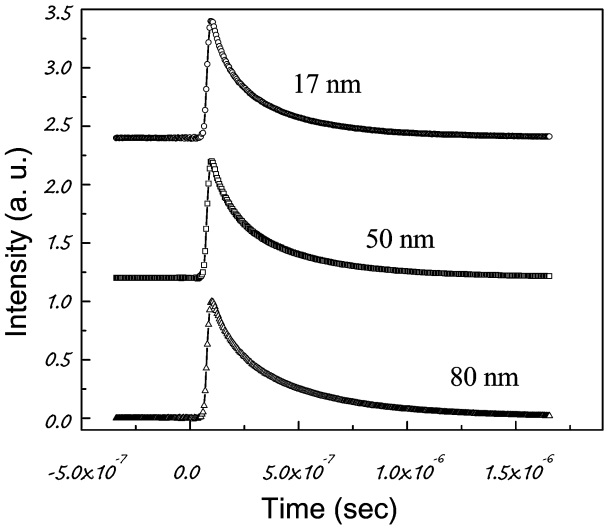

Fig. 3 Photoluminescence decay profiles of films with thickness of 17 (open circles), 50 (open squares), and 80 nm (open triangles). The lines are fits to the data to double exponential decays.

overall rate for the nonradiative process, and three factors may contribute to this parameter:

$$k_{\mathrm{nr}} = k_{\mathrm{decay}} + k_{\mathrm{dd}} + k_{\mathrm{FET}},$$

where k_{decay}, k_{dd}, and k_{FET} are the rates for the nonradiative decay of the triplet MLCT state, crossover to the upper d-d state, and quenching through FET, respectively. k_{decay} and k_{dd} can be presumed to change negligibly by changing thickness since the environment for a molecule can be considered equivalent irrespective of thickness. With FET considered, an inverse cubic dependence of the quenching rate on distance, x, is predicted:

$$k_{\mathrm{FET}} \propto \frac{1}{x^3}.$$

Therefore, the quenching rate is expected to decrease with the distance between a molecule and a surface (either air or glass), resulting in an increase of the lifetime. In this experiment, the samples are layers of finite thickness, and the measured lifetimes should result from an average effect of FET over the distance. The integrated effect of quenching should be considered, but the overall tendency (monotonically increasing lifetime with thickness) is retained.

Lifetimes of the samples with different thickness are plotted in Fig. 4. The lifetime of the short-lived (long-lived) component increases from 80 (329) ns for the 17-nm thick sample to 99 (400) ns for the 200-nm thick sample. This tendency is also in good agreement with the idea described above. In addition, the lifetime seems to approach an asymptote, also consistent with the FET model. Assuming the FET model, an expression for the lifetime of a thin film sample with thickness d can be obtained as follows:

$$\tau_{\mathrm{m}}(d) = \left(\frac{1}{\tau_{\mathrm{r}}} + k_{\mathrm{decay}} + k_{\mathrm{dd}} + \frac{1}{d-d_0}\int_{d_0}^{d}\frac{\beta}{x^3}\mathrm{d}x\right)^{-1} = \left(\frac{1}{\tau_r} + k_{\mathrm{decay}} + k_{\mathrm{dd}} + \frac{\beta}{3}\frac{d+d_0}{d^2 d_0^2}\right)^{-1},$$

where d_0 is a characteristic length corresponding to the distance between the surface and the molecule that is nearest to the surface. For simulation, d_0 was presumed to be 0.82 nm, which is the nearest distance between Ru centers in Ru(bpy)$_3$(PF$_6$)$_2$ crystal.[12] As d approaches ∞, the effect induced by FET becomes smaller as $1/d$ (k_{FET} approaches zero). The

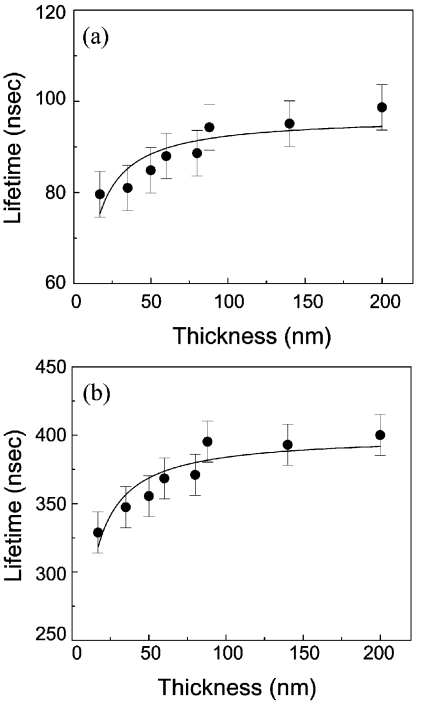

Fig. 4 Lifetime *vs.* thickness plot for (a) the short- and (b) long-lived components. Solid lines are fits using the FET model.

lifetime then approaches the value that is observed under bulk conditions:

$$\tau_{\mathrm{m}}(d \to \infty) = \left(\frac{1}{\tau_{\mathrm{r}}} + k_{\mathrm{decay}} + k_{\mathrm{dd}}\right)^{-1}.$$

According to the fits of these equations to the data in Fig. 4 shown by the solid line, $\tau_{\mathrm{m}}(d \to \infty)$ was found to be 97 ns for short-lived component and 401 ns for the long-lived component.

Although the PL quantum yield could not be obtained from these data because of the absence of a proper reference system, it can be estimated based on the lifetime data for the solution and the thin film. According to the studies on the lifetime of $Ru(bpy)_3^{2+}$ dissolved in different solvents, the radiative lifetime, τ_{r}, is nearly constant and only the rate of the non-radiative process changes with the solvent,[5] an observation that confirms that the radiative decay is the intrinsic process not affected by the environment.[13–15] It can thus be assumed that τ_{r} remains constant irrespective of the phase change from solution to solid. Since the PL quantum yield is described as:

$$\Phi_{\mathrm{PL}} = \frac{\tau_{\mathrm{m}}}{\tau_{\mathrm{r}}},$$

that of the thin film sample can be predicted from a simple ratio of τ_{m} values:

$$\frac{\Phi_{\mathrm{PL,film}}}{\Phi_{\mathrm{PL,solution}}} \approx f_{\mathrm{short}}\left(\frac{\tau_{\mathrm{m,film,short}}}{\tau_{\mathrm{m,solution}}}\right) + (1 - f_{\mathrm{short}})\left(\frac{\tau_{\mathrm{m,film,long}}}{\tau_{\mathrm{m,solution}}}\right),$$

where f_{short} indicates the fraction of the short-lived component, found to be 0.3 in this experiment. Since the PL quantum yield and the lifetime of the triplet MLCT state in acetonitrile are known to be 6.1% and 870 ns,[5] respectively, the PL quantum yield of thin films is predicted to be in the range from 1.8% for the 17-nm thick film to 2.2% for the 200-nm thick film. These values are in agreement with the PL yield estimated from the EL efficiency of single layer devices.[4]

The change in the lifetime (and possibly the quantum yield) induced by the phase-change can be attributed to a difference in the quenching process. As discussed above, the PL lifetime

of a thin film is determined by the non-radiative quenching process that results from three terms, k_{decay}, k_{dd}, and k_{FET}. The lifetime data shown here suggest that FET is responsible for the lifetime change with thickness. k_{FET}, however, approaches zero as the thickness increases, giving a bulk limit value. Moreover, the effect due to k_{FET} results in a small change in the PL quantum yield. Therefore, FET cannot be the main source for the difference in the PL quantum yield between solution and solid phase. The effect of crossover to the upper d–d state (represented here by k_{dd}) can also be ruled out because there is no evidence for a change in the energy gap between the triplet MLCT state and the upper d–d state as a function of phase, although it should be noted that the thermally accessible crossover mentioned is likely to be related to the photostability of $Ru(bpy)_3(PF_6)_2$ in thin films.[5] In thin films used in this experiment, self-quenching can also play a role. Since the degree of self-quenching increases with the number density of a molecule, it is expected to be fairly high in a solid-state sample.[16] Therefore, our data suggest that k_{decay} is enhanced in a solid-state sample because of the self-quenching effect, leading to a lowering of the PL quantum yield. It has been suggested that the degree of self-quenching can be reduced either by adding small amounts of PMMA in the Ru complexes layer[2] or by substituting 5 and 5′ hydrogen atoms to di-*tert*-butyl side chains,[4] resulting in an increment of the PL efficiency (and thus that of EL efficiency).

B. Electroluminescence devices

It has been shown that in OLEDs with ohmic contacts, (such as the $Ru(bpy)_3(PF_6)_2$ devices discussed here[4]), the EL efficiency is determined by the photoluminescence yield of the film.[17] Therefore, it is interesting to explore correlations between the PL yield in the film and the EL efficiency in OLEDs. The evolution of the EL efficiency of ITO/$Ru(bpy)_3(PF_6)_2$/Au devices as a function of the thickness of the $Ru(bpy)_3(PF_6)_2$ layer is shown in Fig. 5. The data were obtained at a 3 V bias and are in agreement with previously reported measurements from our group.[4] The two curves were obtained by testing two different devices on the same film. The two points around 100 nm show a good reproducibility of devices prepared on different samples.

The EL efficiency decreases monotonically from 1% for the sample with the 192 nm thick $Ru(bpy)_3(PF_6)_2$ layer to less than 0.01% for the device with the 46 nm thick layer. This monotonic decrease indicates the absence of strong microcavity effects[18–20] that would cause the efficiency to behave in a non-monotonic way with thickness. This observation is in accord with the low reflectivity of the ITO electrode. The decrease in the EL efficiency is, however, much more dramatic than the decrease in the PL yield of the $Ru(bpy)_3(PF_6)_2$ films on quartz substrates. In the latter samples, the PL yield was estimated to decrease from 2.2 to 1.8% when the film thicknesses varied from 200 to 17 nm. Clearly, additional quenching mechanisms are operating in the OLEDs.

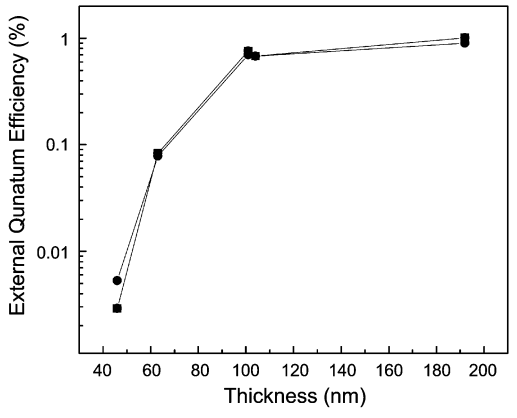

Fig. 5 External quantum efficiency as a function of thickness. Circles and squares are for two different devices fabricated from the same film; the agreement demonstrates reproducibility.

The most important difference between the EL and the PL measurements is the fact that the $Ru(bpy)_3(PF_6)_2$ films in the former have interfaces with ITO and Au rather than with quartz and air. The higher charge density of these conductors will cause more efficient quenching and lead to a more pronounced decrease of the efficiency in thinner devices. In addition to more efficient quenching at the electrodes, triplet–triplet annihilation (TTA) is expected to play a role in determining the EL efficiency.[21] TTA did not play a major role in the PL measurements due to the low excitation density used in the experiments. However, TTA is expected to play a role in the EL efficiency, and especially in thinner devices, due to the higher current (and therefore exciton) density. Our future work will focus on quantifying these effects.

Acknowledgements

This work was supported by the Cornell Center for Materials Research (CCMR), a Materials Research Science and Engineering Center of the National Science Foundation (DMR-9632275), and by the National Science Foundation (Career Award DMR-0094047).

References

1 E. S. Handy, A. J. Pal and M. F. Rubner, *J. Am. Chem. Soc.*, 1999, **121**, 3525.
2 H. Rudmann, S. Shimada and M. F. Rubner, *J. Am. Chem. Soc.*, 2001, **124**, 4918.
3 S. Bernhard, X. Gao, G. G. Malliaras and H. D. Abruña, *Adv. Mater.*, 2002, **14**, 433.
4 S. Bernhard, J. A. Barron, P. L. Houston, H. D. Abruña, J. L. Ruglovsky, X. Gao and G. G. Malliaras, *J. Am. Chem. Soc.*, 2002, **124**, 13 624.
5 K. Kalyanasundaram, *Photochemistry of Polypyridine and Porphyrin Complexes*, Academic Press, London, 1992.
6 P. McCord and A. J. Bard, *J. Electroanal. Chem.*, 1991, **318**, 91.
7 A. W. Knight and G. M. Greenway, *Analyst*, 1994, **119**, 879.
8 N. R. Armstrong, R. M. Wightman and E. M. Gross, *Ann. Rev. Phys. Chem.*, 2001, **52**, 391.
9 L. F. Cooley, C. E. L. Headford, C. M. Elliot and D. F. Kelley, *J. Am. Chem. Soc.*, 1988, **110**, 6673.
10 Because of the wide bandwidth of the light source used in the spectrometer, effects sometimes observed in thin films due to interference were not observed in this work.
11 D. R. Haynes, K. R. Helwig, N. J. Tro and S. M. George, *J. Chem. Phys.*, 1990, **93**, 2836.
12 K. Nagai, N. Takamiya and M. Kaneko, *J. Photochem. Photobiol., A*, 1994, **84**, 271.
13 J. L. Colón, C.-Y. Yang, A. Clearfield and C. R. Martin, *J. Phys. Chem.*, 1990, **94**, 874.
14 E. M. Kober, B. P. Sullivan and T. J. Meyer, *Inorg. Chem.*, 1984, **23**, 2098.
15 J. V. Caspar and T. J. Meyer, *J. Am.Chem. Soc.*, 1983, **105**, 5583.
16 D. P. Rillema, D. S. Jones and H. A. Levy, *J. Chem. Soc., Chem. Commun.*, 1979, 849.
17 G. G. Malliaras and J. C. Scott, *J. Appl. Phys.*, 1998, **83**, 5399.
18 N. Takada, T. Tsutsui,S andSaito, *Appl. Phys. Lett.*, 1993, **63**, 2032–2034.
19 A. Dodabalapur, L. J. Rothberg and T. M. Miller, *Appl. Phys. Lett.*, 1994, **65**, 2308–2310.
20 R. H. Jordan, L. J. Rothberg, A. Dobadalapur and R. E. Slusher, *Appl. Phys. Lett.*, 1996, **69**, 1997–1999.
21 A. Köhler, J. S. Wilson and R. H. Friend, *Adv. Mater.*, 2002, **14**, 701–707.